A control-oriented scalable model for demand side management in district heating aggregated communities

A control-oriented scalable model for demand side management in district heating aggregated communities

Costanza Saletti[a*], Nathan Zimmerman[b], Mirko Morini[a,c], Konstantinos Kyprianidis[b], Agostino Gambarotta[a,c]

[a] *Center for Energy and Environment (CIDEA), University of Parma, Parco Area delle Scienze 42, 43124 Parma, Italy*
[b] *Department of Automation in Energy and Environment, School of Business, Society and Engineering, Mälardalen University, Box 883, Västerås, 72123, Sweden*
[c] *Department of Engineering and Architecture, University of Parma, Parco Area delle Scienze 181/A, 43124 Parma, Italy*

* Corresponding author: costanza.saletti@unipr.it

Abstract

District heating networks have become widespread due to their ability to distribute thermal energy efficiently, which leads to reduced carbon emissions and improved air quality. Additional benefits can derive from novel demand side management strategies, which can efficiently balance demand and supply. However, their implementation requires detailed knowledge of heating network characteristics, which vary remarkably depending on urban layout and system amplitude. Moreover, extensive data about the energy distribution and thermal capacity of different areas are seldom available. For this purpose, the present work proposes a novel procedure to develop a fast scale-free model of large-scale district heating networks for system optimization and control. Each network community is represented and modeled as an aggregated region. Its physics-based model is identified starting from a limited amount of data available at the main substations and includes heat capacity and heat loss coefficients. The procedure is demonstrated and validated on the network of Västerås, Sweden, showing results that are in agreement with data from the literature. Thus, the model is well suited for real-time optimization and predictive control. In particular, the possibility to easily estimate the heat storage potential of network communities allows demand side management solutions to be applied in several conditions.

Keywords: District Heating Network; Demand Side Management; building heat capacity; scalability; gray-box model

1. Introduction

The European Union has recently established long-term objectives to reduce greenhouse gas emissions and, potentially, achieve climate neutrality by 2050, by engaging all sectors of the economy and society [1]. These goals require a complete transformation of the energy system, in which the heating and cooling sector plays a significant role in terms of consumption reduction and potential for decarbonization. Indeed, thermal energy distribution to households and industries can be accomplished by District Heating Networks (DHNs) in a more efficient way compared to individual devices, since they consist of supplying heat produced in centralized plants to the end-users by means of a network of pipelines. Hence, these networks enable the utilization of multiple energy resources, such as renewables, waste heat from industrial processes [2] and storage systems. Moreover, DHNs reduce the number of emission sources, as they move the generation devices based on fuel combustion in centralized sites outside cities and residential zones. For this reason, populated areas, where reduction in carbon dioxide emissions and improvement in air quality conditions are paramount, are ideal for extending this technology to a large scale.

DHNs are already the dominant heat supply systems in some countries such as Sweden and Finland, where they meet about half of the overall thermal demand [3]. In Austria, Poland and Czech Republic the share of heat supply from DHNs is reaches around 25%, while it goes down to less than 5% in southern European countries (e.g. Italy and Spain) [3]. Despite such large differences, research and innovation actions on these topics are widespread across all other European countries, as DHNs have a predominant role in all future decarbonization scenarios [3]. This is confirmed by 58 projects funded by the European Union as part of the Horizon 2020 Framework Programme and which focus on smart district heating systems [4]. Moreover, according to Sernhed *et al.* [5], in Sweden a large number of research projects is being carried out to reduce further energy consumption in DHNs and to promote their application to other areas, while Leoni *et al.* [6] present their research on innovative business models for Austrian district heating utilities.

However, a widespread application of these systems can be challenging [7], as the design, management and control of DHNs vary significantly depending on several factors:

- the geographical area, which defines the typical climate and, therefore, the specific energy demand;
- the system scale [8], which defines the overall demand and the required approach for its representation (i.e. in small-scale systems, consumers can be modeled individually, while in large-scale systems different methods should be used since that level of detail would require a significant computational burden);
- the system configuration and layout, which is becoming more complex due to the need to integrate renewable energy sources;
- the availability of data and information, e.g. energy consumption, building type, weather data and system temperatures.

In order to overcome the aforementioned drawbacks, it is necessary to have reliable models of DHNs, which can be used for different purposes, e.g. design studies, optimization solutions and control-oriented applications. Indeed, it is challenging to perform experimental investigations since proper test rigs are not typically available, due to the system size and characteristic time range. Moreover, demonstration studies of new system configurations and management strategies cannot usually be carried out in real networks, due to the necessity to fulfill the customers' comfort requirements. Furthermore, the comparison of different solutions in real test cases may be inconsistent, as the boundary conditions and disturbances cannot be effectively controlled and are subject to large variations over the year. For these reasons, additional research contributions regarding the improvement of bottom-up energy system models [9] are required to investigate novel management and control solutions and, thus, to make district energy more widespread, energy-efficient and cost-effective.

1.1 District heating models

In the literature there is an increasing number of papers that focus on the development of mathematical models [10] for the simulation of the production, distribution and consumption aspects of DHNs. Figure 1 illustrates the main modeling approaches with a focus on distribution network and heat load.

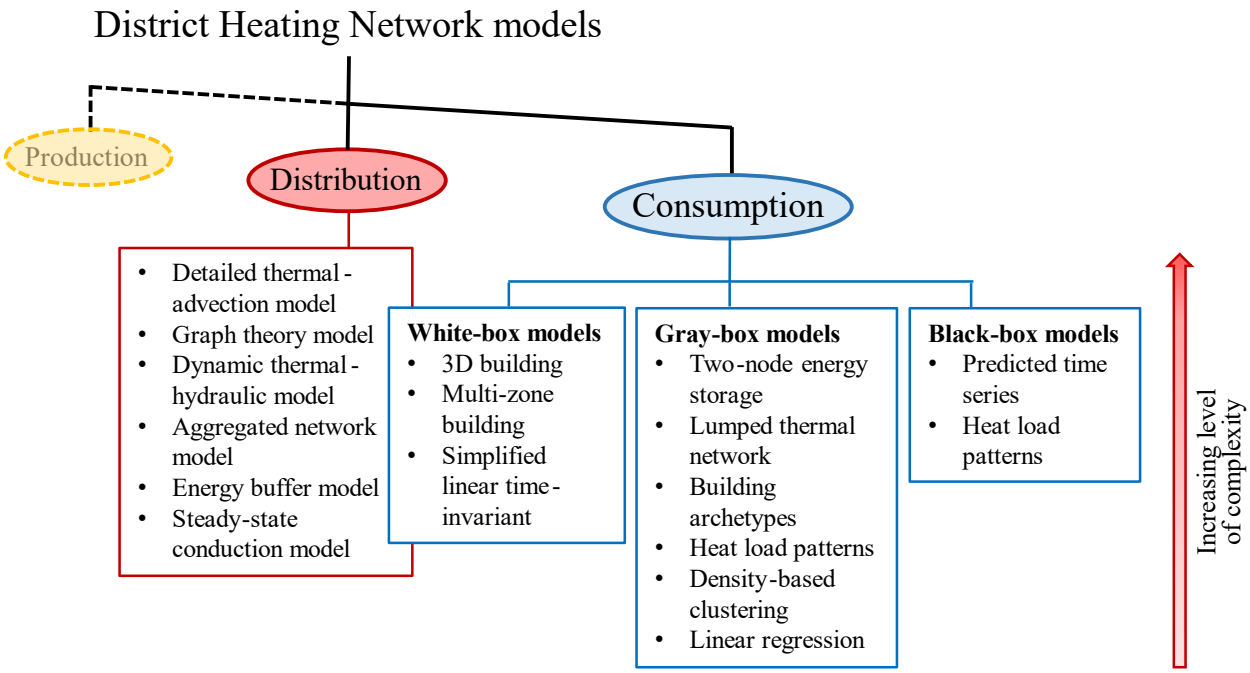

Figure 1. Summary of the main modeling approaches of district heating networks available in the literature: focus on the consumption (and distribution) aspect.

Concerning the district heat load prediction, the most common classification is reviewed by Ma *et al.* [11]:

- Physical models, or white-box models, rely on physical principles and conservation laws (e.g. energy conservation equation), but typically require a significant computational effort, leading to impracticable calculation times in optimization and control applications;
- Statistical models, or black-box models, are based on experimental data and are trained with large datasets, but they do not include a physical representation of the phenomena underlying the system;

- Hybrid models, or gray-box models, are based on a manageable physical representation of the system that relies on empirical relationships obtained from available data giving benefits halfway between the aforementioned modeling approaches.

In the light of this, connected buildings can be modeled with several techniques depending on the level of detail required by the simulation aim. For instance, 3D modeling approaches can be adopted for a detailed representation of the architecture and materials [12]; model order reduction through linearization and simplification allows the model of the building envelope to be scaled into an equivalent model [13]; and building archetypes can be developed and identified through proper representative parameters and construction details [14]. Coakley *et al.* [15] provide an overview of available calibration procedures, which aim to match the output of a building model with measured data. The paper highlights that it is generally difficult to represent the building environment accurately, due to the large number of interacting variables and complex architectures. In addition, the study focuses on individual buildings without considering the connection to district energy systems, and the difficulties in obtaining a fast representation of DHN customers are therefore emphasized. On the other hand, Lundström *et al.* [16] describe a space heating model for existing multifamily buildings, comprising a lumped thermal network (i.e. resistance-capacitance), radiator heating systems and procedures for pre-processing data and boundary conditions. Simulation tests performed on a single-zone building in the Nordic climate show that the model is reliable and computationally fast when compared to detailed building simulation tools. However, information such as building geometrical and thermal properties are required as input data.

In urban districts, the increasing number of buildings leads to significant calculation time and makes it unfeasible to adopt a detailed modeling approach, especially in optimization and control-oriented studies. In this regard, Fonseca and Schlueter [17] combine statistical and analytical methods to cluster buildings in urban neighborhoods and to provide a multi-dimensional model for the investigation of energy efficiency solutions. The work refers to a building archetype database based

on statistical data and adopts detailed geo-referenced information on the analyzed area. Marquant *et al.* [18] propose another density-based clustering method to quantify the potential of DHNs by dividing the city-scale system into smaller subsystems and relying on spatial and temporal aspects of building characteristics. This is done in particular to overcome the limitations of Mixed Integer Linear Programming (MILP) problems, which are exploited in many studies to optimize urban networks [19–21]. Another approach consists of the development of an open source map of heat demand density data for European Union countries, UK, Norway, Iceland and Switzerland [22]. This tool underestimates or overestimates the demand depending on the high or low density of the area, therefore it can be used mainly for preliminary planning analyses.

As regards the distribution network, various models with different levels of detail are employed to represent the system. Some works investigate the transient physical phenomena occurring within the pipelines of DHNs by coupling the detailed hydraulic equations with the thermal advection-diffusion equations, and solving them with an analytic form [23]. While this research introduces significant complexity to the overall system model, another paper [24] aims to further reduce it by aggregating the distribution network and comparing two different methods. One of these allows the number of pipes to be reduced from forty-four to three. Guelpa and Verda [25], instead, propose a compact model that uses the graph theory to represent the topology of large-scale DHNs: each pipe is a branch and each connection is a node. This model does not incorporate the prediction of consumer thermal demand. The same drawback can be observed in other works introducing steady-state system models for DHN planning [26] and dynamic models for topology analysis [27] and sector coupling [28].

1.2 Demand Side Management solutions

One of the most promising key enabling solutions is Demand Side Management (DSM), as it aims to overcome the mismatch between demand and supply [29] through optimal use of existing thermal storage means in the system (e.g. structural thermal mass). The quantification of the DSM and load

shifting potential in DHNs is possible only through the knowledge of the key physical properties of the system.

Despite their suitability for large-scale DHNs, none of the modeling strategies outlined above investigates the potential role of the system heat capacity as storage within optimization and control algorithms, in order to introduce small indoor temperature fluctuations and achieve flexibility through DSM [30]. This application is explored by Yin *et al.* [31], who propose a linear regression model calibrated on data from detailed simulation in order to estimate demand response potential at building level.

Since DHNs, depending on size, comprise a large number of pipelines, some works analyze the water in the networks as thermal storage. For instance, Kouhia *et al.* [32] show that, when the grid is used as storage by allowing the supply temperature to vary freely within certain constraints, the heat provision costs are reduced by 2 %. Moreover, supply temperature optimization is regarded as a promising development to be addressed. Sartor and Dewallef [33] propose to increase the temperature supplied to the DHN up to 140 °C (technical constraint) to mitigate the payback time of additional storage tanks and to improve the operation of the Combined Heat and Power (CHP) plants, which are the most common production units in these systems. The significant increase in heat loss is counterbalanced by a 0.2 EUR/MWh decrease in heat cost due to the avoided use of the backup boilers.

In parallel, other papers analyze the end-users connected to the network as thermal storage [34]. In particular, a study by Dominković *et al.* [35] proposes a building simulation model coupled with a linear optimization model of the DHN in Sønderborg, Denmark, to analyze the benefits of preheating the thermal mass of part of the connected residential building stocks, which are sorted in six archetypes. Hence, data such as floor area, construction age and internal heat capacity are required to replicate the analysis. One of the most relevant studies regarding the thermal inertia of buildings in DHNs is proposed by Kensby *et al.* [36], which presents an actual pilot test performed on five

multifamily residential buildings in order to investigate their potential to serve as short-term energy storage. The selected consumers are equipped with data acquisition devices and subject to five test control cycles, consisting of different periods of charging and discharging. The results are scaled up in order to provide an estimation of the heat storage potential for DHN. Indeed, the authors conclude that an energy amount of 0.1 kWh per square meter of heated floor area causes variations in indoor temperature lower than 0.5 °C in heavy buildings. In a subsequent paper [37], these empirical tests are combined with an energy balance model and a unit commitment problem to compare the use of the building thermal capacity with that of centralized storage tanks. In this case, the former is divided into shallow storage (i.e. radiators and indoor air) and deep storage (i.e. structural elements), which show different rates of heat transfer. This additional level of complexity, which requires the estimation of the model parameters of these types of storage, might hinder its application to other contexts.

An interesting approach is proposed by Bhattacharya *et al.* [38], who generalize information from the consumers located downstream each main substation and, based on this, create a substation model of low complexity, in order to reduce the dimensionality of a network optimization problem. Then, they present successful demand response strategies based on such a hierarchical architecture. Nevertheless, it is assumed that the substation managers know the building thermal parameters, which have to be investigated through a dedicated data-driven technique [39].

Similarly, other studies investigate both the network and consumers as potential heat storage devices. It is oftentimes specified that the latter is a more feasible solution, but the required individual analysis of the DHN and building construction characteristics [40] can be time-consuming and often inaccurate (since such parameters are not always well-known). An integrated approach to the operational optimization of DHNs that includes all three types of storage (i.e. hot water tanks, thermal inertia of pipelines and thermal inertia of buildings), but not real-time control, is proposed in [41].

Recent control-oriented studies manage to reduce thermal imbalance between heat users by means of an online prediction and indoor temperature feedback method [42], to lower the operating temperatures of the network [43] or to maximize the utilization of industrial waste heat [44]. In all these strategies, the consumer heat load is provided by means of other techniques and cannot be varied to integrate DSM. This is mainly due to system complexity [45] and lack of fast and suitable modeling approaches.

On the other hand, a promising control application is shown in [46] by the authors of the present paper. A novel controller based on Model Predictive Control (MPC) operates DSM in a large-scale DHN by storing heat within the heat capacity of the end-users to improve network operation. For this purpose, the different communities of the network are considered as thermal batteries with a maximum storage capacity. The MPC varies the State of Charge of these batteries in an optimal way and achieves up to 16 % reduction in the demand peaks and up to 20 % reduction in heat loss from the distribution pipelines. This application, however, requires a compatible model that contains physical information of district heating aggregated communities (e.g. heat capacity and loss) in order to estimate their DSM potential and build the State of Charge.

The available consumer models outlined in the previous sections are summarized in Table 1 with their main features, advantages and disadvantages. It emerges that, while models with a higher degree of complexity can be used for faithful simulation of DHN consumers, they cannot be exploited for applications where a low computational time is paramount, such as DSM and advanced control strategies, which require the model to be computed many times within a relatively short time frame in the search for an optimal or at least sub-optimal control law.

Therefore, it is necessary to develop a complete modeling procedure, not available in the literature, to extract key information on the system main dynamics in order to enable real-time DSM.

Table 1. Summary of literature models of the consumers in district heating networks and their main features.

Paper	Modeling technique	Model type	Key equations and details	Key applications	Inclusion of heat capacity	Suitability for DHNs	Advantages	Disadvantages
[12]	3D building model	White-box	Physical model of building zones and HVAC system	Calibration, identification of energy saving techniques	Yes	No	High level of detail and accuracy	Information on building properties and layout required
[34,35]	Multi-zone model	White-box	Zone physical model with heat transfer phenomena	Energy flexibility and demand response evaluation	Yes	Yes	High level of detail	Building properties required, high computational time
[13]	Simplified linear time-invariant	White-box	State-space representation of physical phenomena	Urban energy simulation	No	Yes	Good trade-off accuracy computational time	Information on building properties required
[14]	Building archetypes	Gray-box	Parameters representative of key physical variables	Building retrofit, optimize regulation	No	No	Reduction of required parameters	Large housing database required, not necessarily representing all house types
[16]	Lumped thermal network	Gray-box	Resistance-capacitance network equations	Energy planning and management	Yes	No	Low computational time, good accuracy	Information on building properties required
[17]	Energy consumption patterns	Gray-box	Physical model of building zone coupled with statistical aggregation analysis	Analyze energy efficiency measures	No	Yes	4D visualization of district heat load patterns allowed	Geographic information system required
[18]	Density-based clustering	Gray-box	Homogeneity index to represent cluster load profile	Large-scale modeling and MILP optimization	No	Yes	Fast resolution of large optimization problems	Building energy demand profiles required
[31]	Linear regression model	Gray-box	Linear equation fitted on data from detailed physical model	Demand response potential prediction	Yes	No	High level simulation not needed	High level simulation needed for different building types
[37]	Two-node energy storage system	Gray-box	Hourly thermal energy balance	Unit commitment problem with thermal energy storage	Yes	Yes	Fast applicability to optimization problem with heat storage	Tuning of model parameters required
[41]	Heat load as predicted time series	Black-box	-	Network optimization, demand side management	No	Yes	Fast resolution of large optimization problems	Prediction method required, no correspondence with physical phenomena
[47]	Heat load pattern	Black-box	-	Discovery of typical and atypical behavior in DHNs	No	Yes	Large-scale automatic analysis allowed	Large dataset required, no correspondence with physical phenomena

1.3 Scope and contribution of the work

As mentioned above, the state-of-the-art research on DHNs lacks simplified models of DHN communities with all three following features:

- They are control-oriented, suitable in particular for online optimization and optimal control applications;
- They include heat capacity estimation suitable for DSM;
- They can be applied to large-scale DHNs without the need to carry out extensive and detailed investigations of the network characteristics and individual building data, which can be time-consuming and often inaccurate.

In order to address this research gap, the present paper proposes a novel procedure to build a reduced-order, scale-free model of DHN aggregated end-users by means of a limited amount of data, which are usually available from the system substations, and with a small set of assumptions. The procedure does not depend on the scale of the system, as it merges and aggregates the dwellings connected to the substation regardless of their specific characteristics and dynamic response. Other studies introduce aggregation approaches of DHN areas for system design and integration in urban contexts [48], but not for DSM and control.

The proposed hybrid solution combines data-driven knowledge with a physics-based approach to evaluate the main parameters of the connected communities, which incorporates their heat capacity and heat losses to the environment. This simplifies the district modeling procedure to a great extent, making it accessible to district heating utilities without specific modeling competences and without requiring system knowledge with a fine granularity. The obtained gray-box model can then be used to implement MPC and achieve a higher system efficiency as demonstrated in [46].

The method is tested on the district heating network of the city of Västerås, in central Sweden. Nonetheless, it is applicable to substations supplying entire regions (without detailed information on the utilization units) as well as individual buildings.

2. Model development

This section details the research method presented in this paper for the development and identification of a control-oriented model that includes the estimation of heating network dynamic parameters in order to enable DSM. A schematic illustration of the method is given in Figure 2.

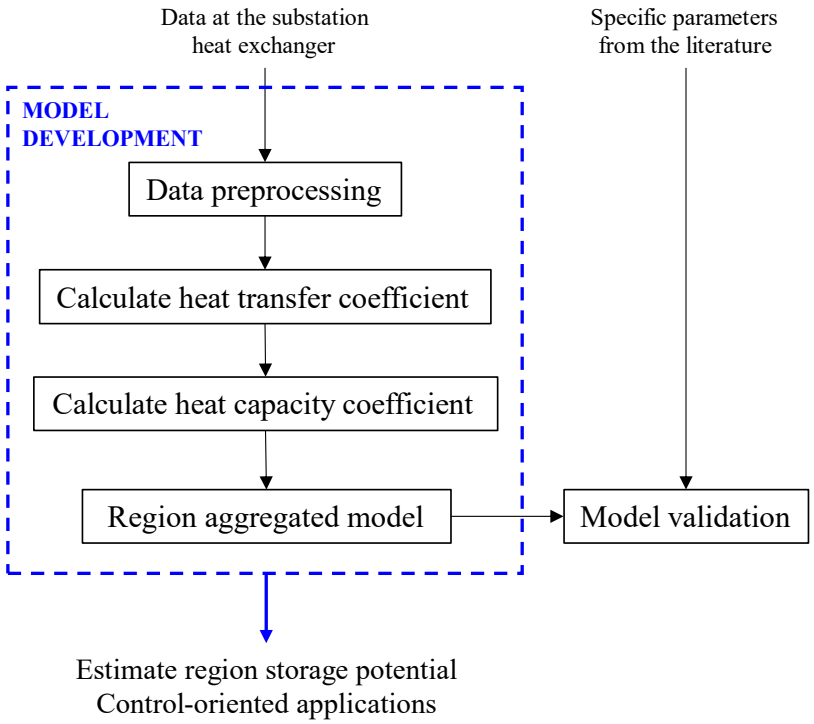

Figure 2. Block diagram of the method for the aggregated region model development.

The aim of the model is to represent a generic area of a district heating network supplied by a substation heat exchanger, regardless of the number, topology or type of the connected buildings, starting from the data available from the given substation. The considered dataset is analyzed and preprocessed in order to eliminate odd values and outliers (Section 2.1). Then, it is used to identify the relevant coefficients of a simplified model that represents the given aggregated set of consumers (i.e. aggregated region) and considers both their heat loss and heat capacity (Section 2.2). The application and verification of this procedure to the main substation heat exchangers of a large-scale DHN is carried out in Section 3, together with sensitivity analysis on the model coefficients. Then, the obtained values are compared with specific coefficients per unit of heated area or heated volume,

typically related to individual buildings connected to DHNs, available in the literature [37,49]. This represents the model validation with literature parameters (Section 4).

2.1 Data preprocessing

In many countries such as Sweden, district heating providers are required to measure heat consumption through smart meter devices installed in the substations. The availability of data makes it possible to identify the usual behavior of the system to a greater extent and to investigate more efficient management strategies. For instance, Calikus *et al.* [47] perform a data-driven investigation of the heat load pattern of two district heating networks in southern Sweden in order to provide a better understanding of typical and atypical customer behavior depending on their category. However, it is still common that in other contexts the data acquisition devices are only installed in given sections of the network. Hence, as mentioned in Section 1, it is beneficial to investigate methods that can be implemented in networks where the end-users are not monitored at an individual building scale.

Moreover, since the data are collected automatically [47], there might be connection issues resulting in missing data or values that are not significant in the dataset. Hence, a proper preprocessing phase is carried out to remove the acquisitions corresponding to missing sensor readings.

Generally, the datasets available at the substation heat exchangers include the following quantities:

- water mass flow rate of the primary side of the substation heat exchanger, $\dot{m}$;
- supply and return temperature of the primary side of the substation heat exchanger, T_S and T_R, respectively;
- outdoor temperature, T_{ext}.

Therefore, the thermal power actually transferred to each region $\dot{Q}$, which covers the heat demand of the aggregated end-users, can be calculated according to the energy balance in Eq. (1):

$$\dot{Q} = \dot{m} \cdot \mathrm{c} \cdot (T_{\mathrm{S}} - T_{\mathrm{R}}) \quad (1)$$

where *c* is the water specific heat capacity.

In other cases, the thermal power or the heat supplied over a given time interval are available from heat meters. The following procedure is applicable as long as the thermal power can be derived.

Since this analysis aims to create a model that is suitable for exploiting the heat capacity of the consumers when there is a significant thermal demand, e.g. to implement DSM strategies in presence of thermal peaks, the data referred to heating seasons (i.e. from October of each year to March of the following year) are extracted from the initial dataset.

In addition, other conditions in which the collected heat demand is low and which are usually far from the typical pattern of a heating season are excluded. For this purpose, days during which acquired data show one of the following features are eliminated from the dataset:

- the thermal power is zero or negative;
- the supply temperature is lower than a given threshold (e.g. 40 °C);
- the difference of temperature at the primary side of the substation is lower than a threshold (e.g. 10 °C);
- the outdoor temperature is higher than 19 °C.

The presence of such cases in the dataset might be due to failures in the measurement equipment or connection.

2.2 Model identification

The model identification procedure is similar to that proposed by Guelpa *et al.* [49], who adopt a clustering approach in order to identify the relevant characteristics of the buildings in the DHN of Turin, Italy. They calculate the coefficients that characterize a compact model based on the energy balance of each building starting from seasonal data.

In the present work, firstly the data are visualized in order to identify load profiles and typical behaviors. Generally, each day of the heating season shows a double peak behavior in heat load, in which the load increase in the early morning is followed by a maintenance period and then a second peak in the evening. Then, without other information concerning the individual end-users and the network specific configurations, the dataset related to each region is used to identify a simplified dynamic model that represents the sum of the buildings of the given area as a single aggregated consumer, depicted in Figure 3. For this purpose, the region is considered as a system with a given mass at a uniform temperature T, which is an equivalent representation of the energy content of the aggregated consumer.

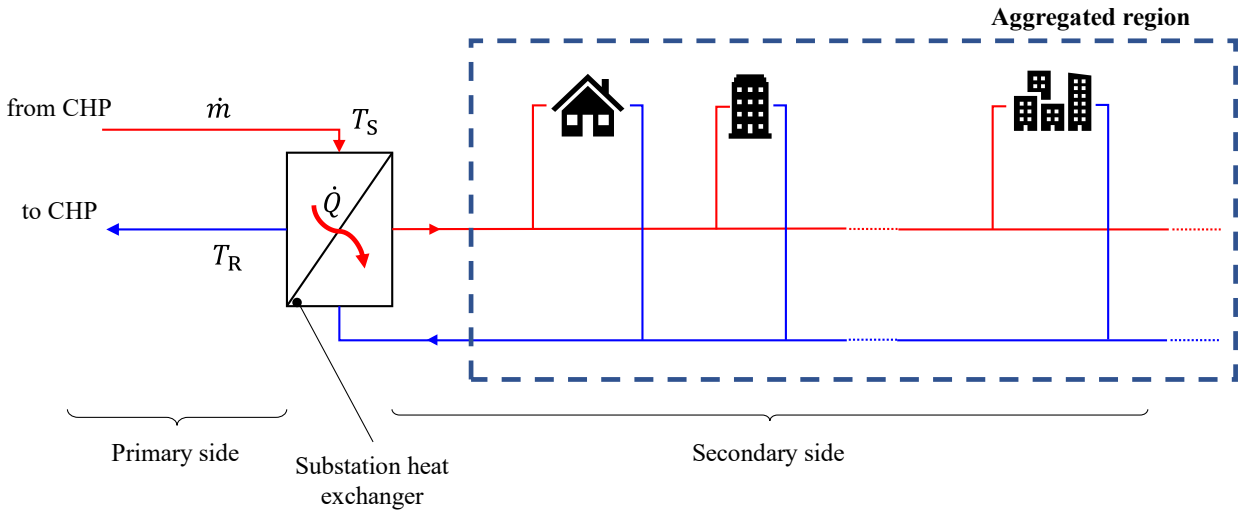

Figure 3. Schematic representation of the assumption of aggregated region adopted in the work. The data available at the substation heat exchanger of the aggregated region are water mass flow rate $\dot{m}$, supply and return temperature T_S and T_R, respectively and, consequently, thermal power $\dot{Q}$ transferred to the region.

A simplified and reliable representation of the aggregated consumer has to consider the main factors that affect its thermal behavior, which are (i) the heat dissipation through the envelope – determined by the difference between indoor and outdoor temperatures – and (ii) the thermal power supplied by the DHN. The model is represented by the thermal balance in the following form:

$$\frac{dT}{dt} = -\frac{U}{C}(T - T_{\text{ext}}) + \frac{1}{C}\dot{Q} \quad (2)$$

where T_{ext} is the outdoor temperature and $\dot{Q}$ is given by Eq. (1). The aggregated heat transfer coefficient U and the aggregated heat capacity C of the region are the relevant parameters of the model. It is worth stating that the energy needs of all connected buildings contribute to the heat demand of this aggregated consumer and, consequently, influence the collected dataset. Thus, the results of the model identification procedure based on such dataset reflects the merged properties of the buildings, regardless of their size and dynamic response. Furthermore, this assumption reduces the influence of the behavior of atypical buildings such as differently-sized spaces (difficult to model individually at district scale), even when deviating from the average.

The procedure for the calculation of the model coefficients from the available data is described in the following sections.

2.2.1 Calculation of the heat transfer coefficient

In the most part of large DHNs, actual indoor temperatures are rarely acquired, and significant mean values are difficult to estimate. Thus, the heat transfer coefficient U is calculated by assuming that the indoor thermal conditions of the aggregated consumer are constant, with an equivalent temperature equal to 21 °C [50], for given periods over the day, as described below. Eq. (3) is obtained and calculated for each data point of the dataset.

$$U = \frac{\dot{Q}}{(T - T_{\text{ext}})} \quad (3)$$

The mean of the obtained values gives the estimation of the average coefficient U.

Four different calculation methods are compared to challenge the reliability of the assumption:

- **Method 1**: all data related to the heating seasons are selected for the calculation of the average *U*.
- **Method 2**: the data corresponding to the maintenance phase on weekdays, in which the indoor comfort conditions of the buildings are kept constant [49] due to building occupation, are selected for the calculation of the average *U*. This typically corresponds to late morning and afternoon, e.g. hours from 10 a.m. to 6 p.m. In residential dwellings this maintenance phase can last longer, however, the present model includes different types of end-users, such as commercial and education buildings. Hence, the assumption of constant indoor temperature is presumably more reliable during the hours of the day mentioned above, in order to include all users.
- **Method 3**: the data corresponding to the days on which the percentage variation between maximum and minimum daily thermal power is close to the percentage variation between maximum and minimum indoor-outdoor temperature difference are selected for the calculation of the average *U*. This means that the daily variation of the outdoor temperature can potentially justify the daily variation of the heat load as well as the initial assumption.
- **Method 4**: both sides of Eq. (3) are integrated in order to obtain the coefficient as the integral mean over each day. The average of these values over the heating season is selected for the calculation of the average *U*.

The results given by these calculations are discussed in the light of the results of the case study presented in Section 3. The method that is expected to better comply with the initial assumption of constant indoor temperature over a daily maintenance phase is method 2. In any case, once the heat transfer coefficient *U* has been selected, it is possible to proceed with the model identification.

2.2.2 Calculation of the heat capacity coefficient

Starting from the estimation of the equivalent heat transfer coefficient calculated above, the heat capacity *C* is evaluated by assuming that the indoor temperature of the aggregated region is subject to periodic variations over the days. For instance, in most buildings in Sweden the indoor temperature set-points are kept at 21 °C during the day while a set-back temperature of 17 °C is fixed during the night [50]. The typical daily profile of the indoor building temperature is subject to an increase up to approximately the former temperature and then a decrease to the latter. It is reasonable to assume that the evolution of the region equivalent temperature over each day resembles this profile.

The coefficient of each region is estimated by solving the following optimization problem:

- The equivalent indoor temperature of the aggregated consumer is simulated with the input data over a defined period as a function of *C*.
- The temperature has to be maintained within the set-point and set-back boundaries (i.e. $T_{\mathrm{SP,max}}$ and $T_{\mathrm{SP,min}}$, respectively), which can vary over the day. For this purpose, a cost function that considers the total heat-degree-hours over the simulation period for which the temperature, as a function of *C*, is higher than $T_{\mathrm{SP,max}}$ or lower than $T_{\mathrm{SP,min}}$ is evaluated as follows:

$$J(C) = \int \max\left(0, T(C,t) - T_{\mathrm{SP,max}}\right) dt - \int \min\left(0, T(C,t) - T_{\mathrm{SP,min}}\right) dt + \sum_{k} \phi\, f_{\mathrm{k}}(C, [t_{\mathrm{k}}, t_{\mathrm{k+1}}]) \quad (4)$$

- Since the temperature also has to show a variation over each day, the maximum and minimum temperatures reached during each day shall lie within given acceptability bands (e.g. 20 °C to 22 °C and 17 °C to 18 °C for the maximum and minimum temperatures, respectively). A feasible daily behavior of the equivalent indoor temperature, with its extreme values contained within the acceptability bands, is shown in a qualitative way in Figure 4. The width of the acceptability bands inherently considers in the aggregated model the behavior variability of different buildings within a region. The set-point and night set-back temperatures as well as

the width and position of the acceptability bands can be defined in accordance with the regulations or typical conditions of the country in which the system under analysis is located.

- For each *k*-th day, a flag variable f_k is assigned, which is equal to 0 if the constraints described in the previous point are met, and equal to 1 otherwise. This means that, for each day in which the equivalent temperature, as a function of *C*, does not match the given acceptability bands ($f_k = 1$), a penalty factor ϕ (e.g. 10^6 °C s) is added to the cost function $J(C)$. In this way, the solution of the optimization problem is pushed away from unacceptable values of *C*.
- The cost function $J(C)$ is minimized and, therefore, the value of *C* that leads to the most reasonable behavior of the system is obtained.

This procedure is adopted to guarantee that the value of *C* is coherent with the expected daily periodical variation. A low value of heat capacity leads to sharp oscillations in the temperature and, consequently, to the underestimation of the storage potential of the given region. On the contrary, a high value of the coefficient leads to a nearly constant temperature behavior and to the overestimation of the storage capability. This, in turn, leads to the underestimation of the effects on the end-users of various management choices.

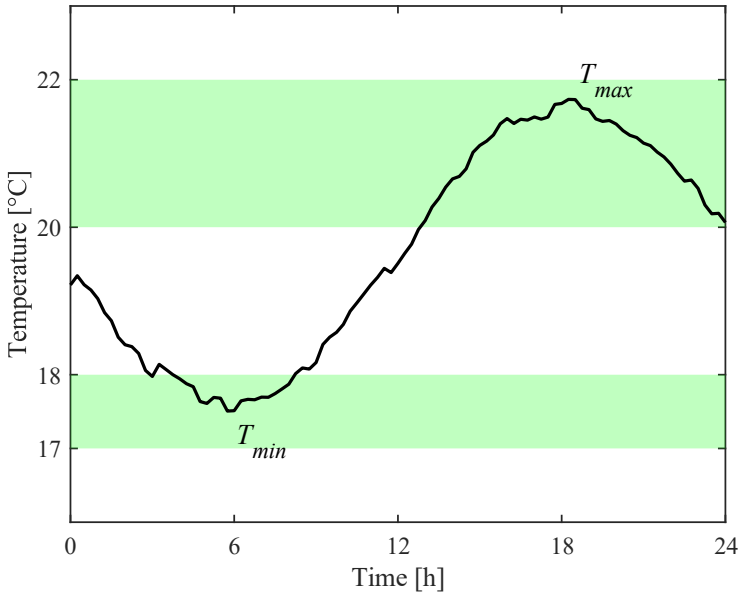

Figure 4. Qualitative representation of a feasible daily behavior of the equivalent indoor temperature of the aggregated region. The shaded areas are the acceptability bands for the maximum and minimum daily values.

3. Results

In this section, the procedure described in Section 2 is evaluated through its application to a case study, which is the large-scale DHN of the city of Västerås, in the Västmanland county, in central Sweden. After a description of the case study and the available dataset, the obtained results are presented and assessed through sensitivity analysis. Since the method has been described in a generic way, its further extension to different systems, sizes and applications is straightforward.

3.1 Case study description

The Västerås DHN is supplied by a centralized production site, comprising a waste-to-energy CHP plant, back-up boilers and thermal energy storage tanks. Six peripheral regions within the area are supplied by the DHN: Surahammar, Skultuna, Rönnby, Tillberga, Barkarö and Hallstahammar. Historical data are collected from the main substation heat exchangers of the six external regions during the period January 2016–May 2019, with a resolution of one hour. The acquisitions regard the water mass flow rate, supply temperature and return temperature. Hence, the hourly thermal power provided to each region can be derived from Eq. (1).

The entire thermal power dataset together with the outdoor temperature are illustrated in Figure 5. It can be noted that, as expected, the thermal demand in the summer months in significantly lower than in winter. This justifies the selection of the heating seasons for the model development phase, as indicated in Section 2.1. It has to be stated that the regions of Surahammar and Skultuna show a flat pattern during 2016 and during 2016 and 2018 to 2019, respectively. As a matter of fact, the data collection campaigns may be subject to several issues, such as potential faults in the metering system or data communication protocol, which are accurately classified in [51]. Furthermore, it is underlined that district heating utilities encounter significant difficulties in identifying and solving faults and deviations [51]. Thus, it is paramount to show that the presented procedure is feasible in realistic conditions, including datasets with low quality.

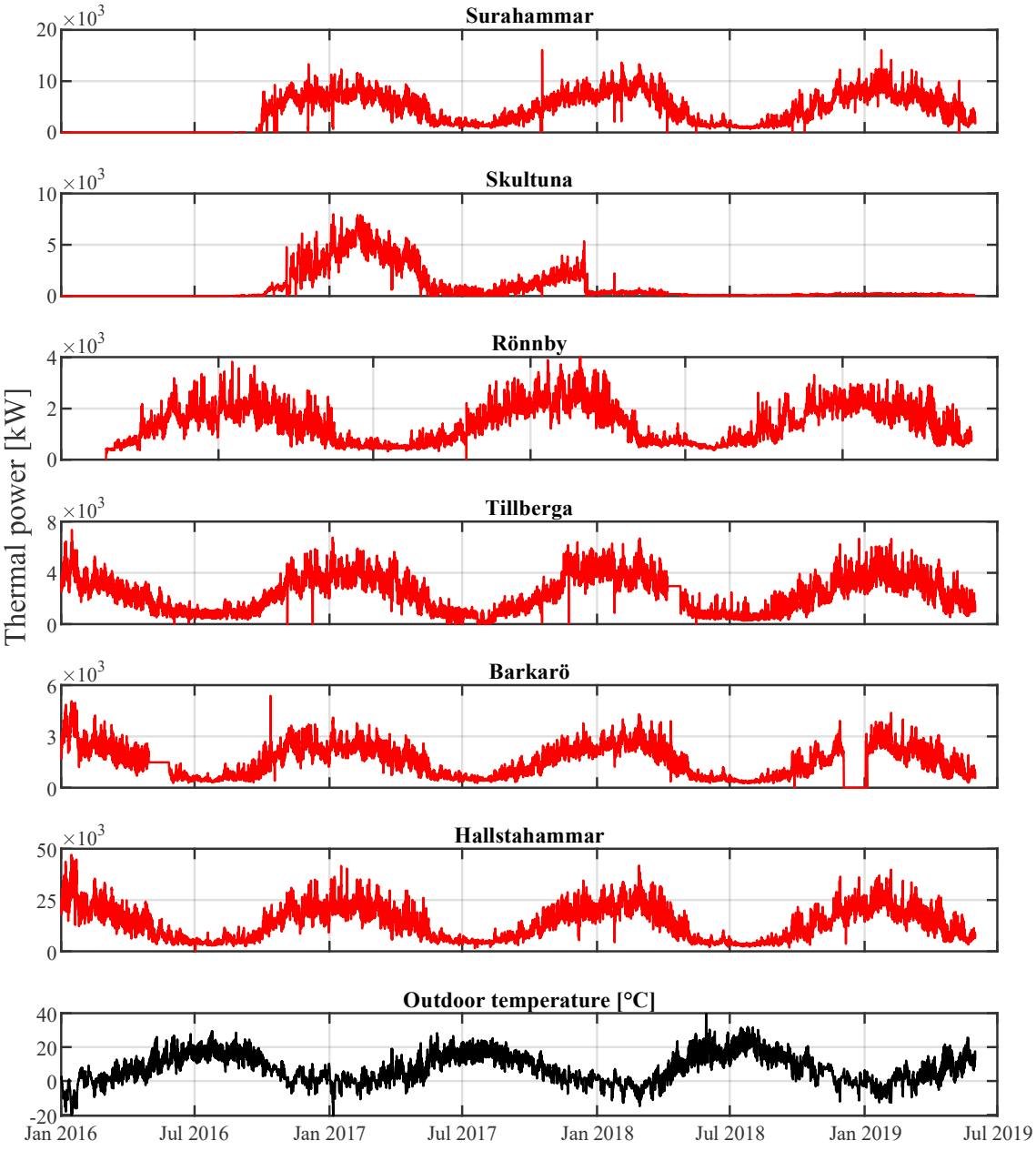

Figure 5. Original dataset of outdoor temperature and thermal power transferred to the regions.

For this reason, it is worth reporting also an illustrative dataset deriving from the automatic preprocessing procedure of a region characterized by incomplete data due to real-world faults. The data of thermal power, mass flow rate, and supply and return temperature related to one heating season of Surahammar, chosen as an illustrative example, are reported in Figure 6, after being preprocessed. It is verified also in this case that, while the outdoor temperature decreases, the thermal power increases almost symmetrically, as a consequence of a higher demand to keep end-user comfort.

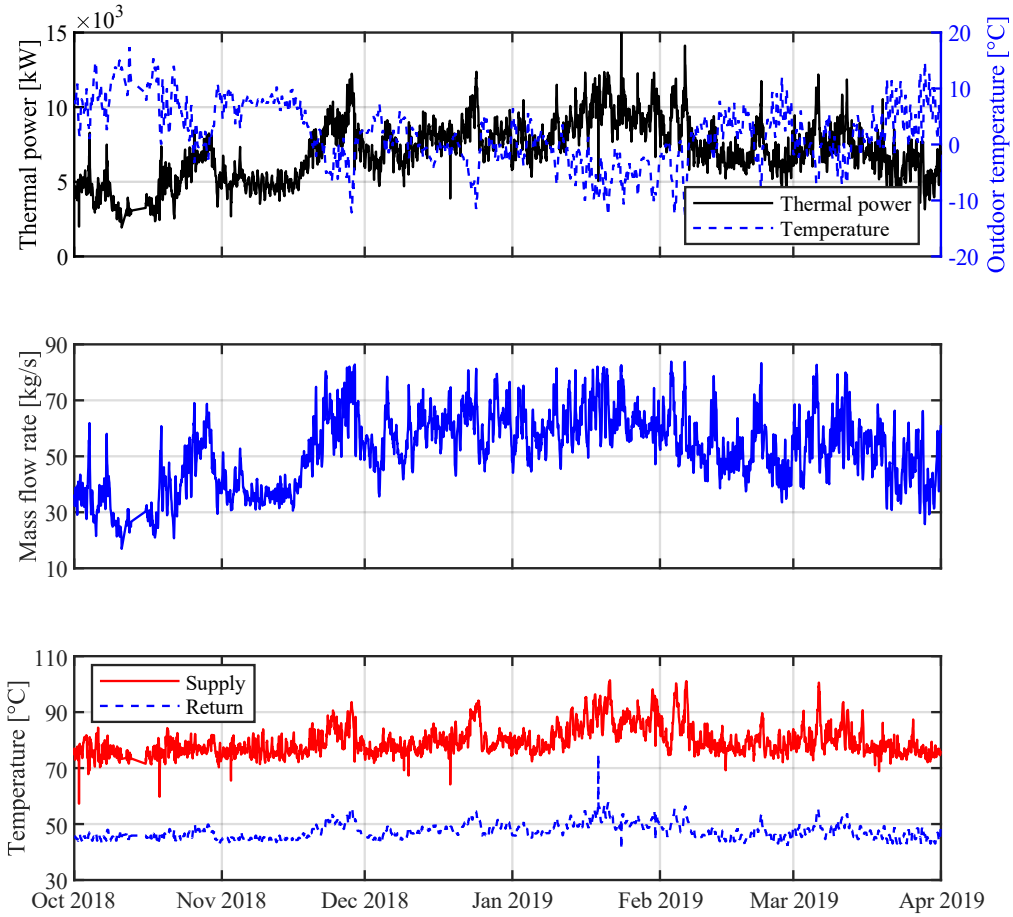

Figure 6. Thermal power, outdoor temperature, mass flow rate, and supply and return temperatures of the region of Surahammar during the 2018–2019 heating season.

The original datasets of all six regions are cleaned by means of the automatic procedure according to the preprocessing criteria listed in Section 2.1. All heating seasons (October-March), if they respect the mentioned criteria, are extracted. Finally, the resulting new dataset of each region is used to identify the parameters of the model in Eq. (2) representing its thermal behavior.

3.2 Identification results

The model identification procedure consists of calculating, for each aggregated region, firstly the heat transfer coefficient and, once its value has been selected, solving the optimization problem that calculates the heat capacity coefficient.

As regards the heat transfer coefficient *U*, the results obtained with the four methods (see Section 2.2.1) for the six regions of the network are reported in Table 2. The average values and standard deviations (absolute and relative to the average) are also shown. It is possible to notice that the standard deviation is lower than 8 % in all cases, so all the methods can be considered almost equivalent. However, methods 1 and 4 tend to return lower values of the coefficients. This might be due to the fact that it is not consistent with the assumption of constant indoor temperature to consider all the daily measurements. On the other hand, the hypothesis of constant indoor temperature only during the maintenance period is expected to better represent the behavior of the buildings over the day. Thus, the coefficients obtained with method 2 are used to proceed with the model identification. Moreover, it is more convenient to overestimate the coefficient that affects the heat losses to the environment, in order to reduce the risk of adopting new DMS solutions that do not comply with the comfort requirements.

Table 2. Calculation of the heat transfer coefficient *U* (in [kW/°C]) for all six regions with four different methods. The average value and standard deviation are also shown.

Region	Method 1	Method 2	Method 3	Method 4	Average	Standard deviation	Standard deviation
	[kW/°C]						[%]
Surahammar	367.2	390.2	392.0	366.8	379.0	13.9	3.7
Skultuna	219.4	239.5	250.4	218.7	232.0	15.6	6.7
Rönnby	99.3	101.8	101.9	99.3	100.6	1.5	1.5
Tillberga	177.0	200.3	201.6	176.6	188.9	13.9	7.4
Barkarö	114.3	117.0	117.0	114.2	115.6	1.6	1.4
Hallstahammar	1046.0	1104.7	1106.6	1046.0	1075.8	34.5	3.2

The subsequent calculation of the heat capacity coefficient *C* is carried out with the following parameters:

- set-point and set-back temperatures of 21 °C and 17 °C, respectively, according to the typical conditions in Sweden presented in Section 2.2.2;
- acceptability bands for the maximum daily temperature between 20 °C and 22 °C, and for the minimum daily temperature between 17 °C and 18 °C.

The results of the estimation of the heat transfer coefficient *U* and heat capacity coefficient *C* of the Västerås DHN regions are reported in Table 3.

The identification procedure has been demonstrated on six regions under the assumption that there is no additional knowledge on the type of end users, in order to make it potentially replicable to any substation. In any case, if additional system knowledge is available for a specific substation (e.g. share of constituent building types, building occupation, typical set-point temperature), it is possible to customize the related parameters of the method (e.g. set-point or night set-back temperature, width of the acceptability bands, length and time of the maintenance phase).

Table 3. Estimation of the heat transfer coefficient and heat capacity coefficient for the six regions of the Västerås district heating network.

Region	U [kW °C^{-1}]	C [kJ °C^{-1}]
Surahammar	390.2	$13.750 \cdot 10^6$
Skultuna	239.5	$11.974 \cdot 10^6$
Rönnby	101.8	$5.350 \cdot 10^6$
Tillberga	200.3	$10.550 \cdot 10^6$
Barkarö	117.0	$3.875 \cdot 10^6$
Hallstahammar	1104.7	$39.350 \cdot 10^6$

3.3 Sensitivity analysis

The robustness and reliability of the procedure for estimating the parameters *U* and *C* with a feasible margin of error is assessed through sensitivity analysis. For this purpose, the six aggregated regions

of the Västerås DHN are simulated for three representative days of January: this means that the model equations of the regions represented by Eq. (2) are integrated with, as inputs, the historical data of thermal power and outdoor temperature for the given period. The simulations are carried out firstly with the calculated coefficients and then with the coefficients that are increased and decreased by a given percentage, in order to show their influence on the behavior of the model. Figure 7 represents the equivalent indoor temperature when the heat transfer coefficient *U* is varied by ±10 % while Figure 8 represents the equivalent temperature when the heat capacity coefficient *C* is varied by the same percentage. Since the standard deviation of *U* calculated with different methods (Table 2) is lower than 8 % in all cases, it is reasonable to assume that value as an uncertainty parameter.

The results show that an increase in *U* has a greater effect on the behavior of the model than an equal increase in *C*. Thus, the margin of error on the former is smaller than on the latter. Nevertheless, *U* has been estimated with good confidence by the fact that different methods lead to similar outcomes.

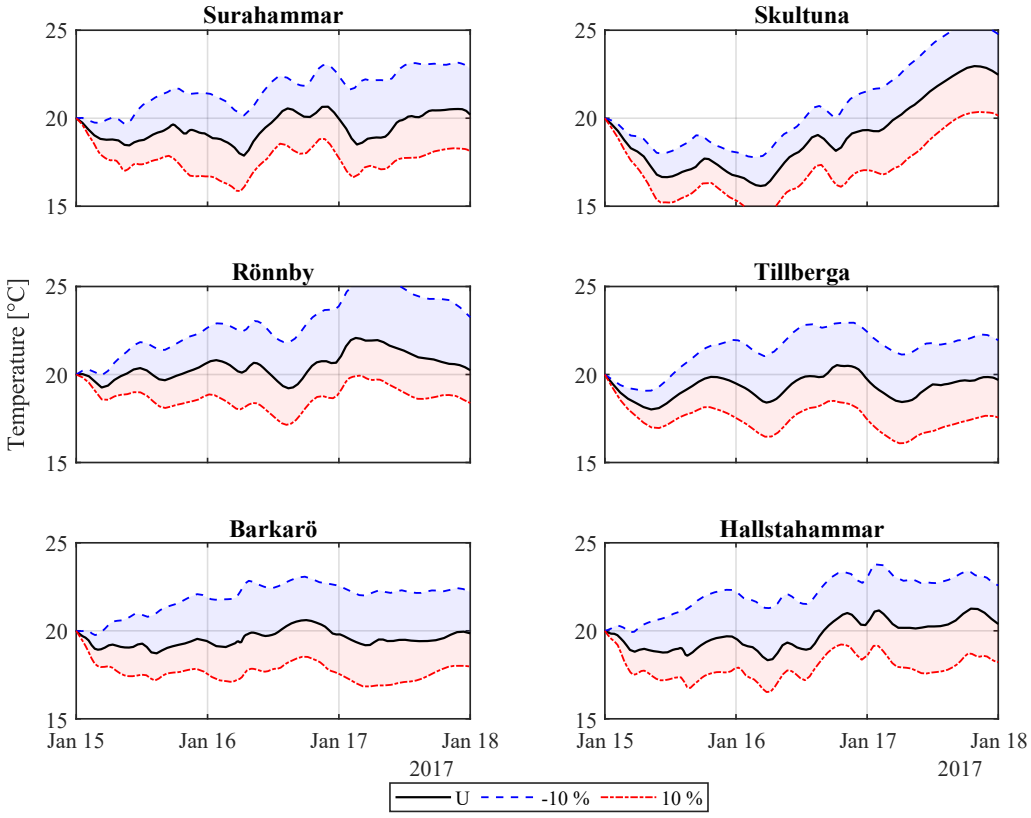

Figure 7. Sensitivity analysis of the behavior of the model with the heat transfer coefficient *U*, considering a ±10 % variation.

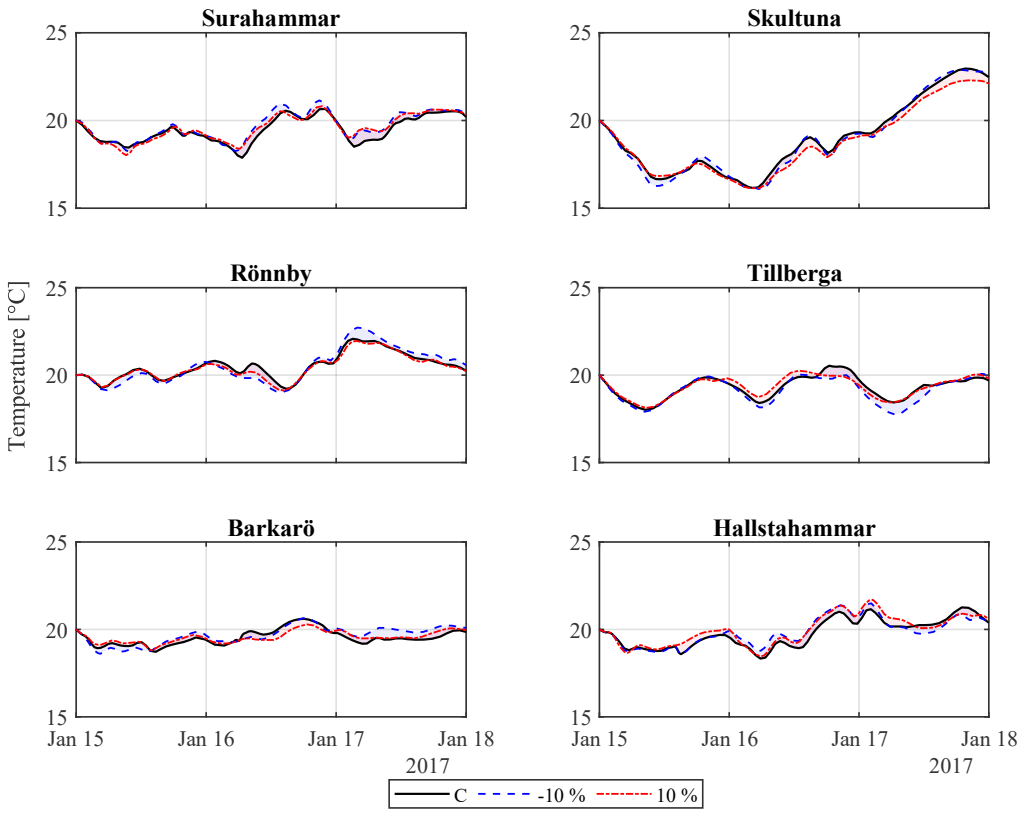

Figure 8. Sensitivity analysis of the behavior of the model with the heat capacity coefficient *C*, considering a ±10 % variation.

Additionally, it is possible to state that the calculated coefficients (Table 3) lead to an acceptable behavior of the equivalent temperature (full lines), while the curves obtained with lower and higher values of *U* (dashed and dashed-dotted lines, respectively) tend to diverge due to the dynamic nature of the model. The effect of varying the heat transfer coefficient is reduced when the outdoor temperature is higher (e.g. autumn and spring). This is given by the fact that the rate of variation of the temperature is proportional to *U* and to the difference between the equivalent temperature and the outdoor temperature (Eq. (2)). For this purpose, Table 4 reports the average deviation between -10 % and +10 % curves (Figure 7) in three different seasons, showing a significantly lower deviation (obtained with higher and lower values of *U*) during middle seasons.

On the other hand, the deviation obtained by varying the heat capacity coefficient as presented above is not appreciable. The influence of this parameter is further explored by increasing and decreasing it by up to one order of magnitude. For this purpose, Table 5 reports the maximum and minimum value,

and the maximum difference of the equivalent temperature profile of Surahammar, taken as example. As expected and mentioned in Section 2.2.2, a lower *C* leads to significant daily temperature variations (i.e. up to two times higher than that obtained with the calculated baseline coefficient), while a higher *C* leads to a flat temperature profile. Since both conditions are not acceptable, the calculated value of *C*, which leads to daily temperature oscillation with an amplitude of around 2 °C to 3 °C, is considered reasonable for the presented model.

Table 4. Influence of the heat transfer coefficient *U* on the behavior of the model: average temperature deviation in [°C] between the two temperature curves (i.e. -10 % and +10 %) on three representative days in different seasons.

Region	November [°C]	January [°C]	March [°C]
Surahammar	2.98	4.02	2.42
Skultuna	2.00	3.61	2.41
Rönnby	2.69	4.18	2.18
Tillberga	2.72	3.95	2.26
Barkarö	3.40	4.20	2.54
Hallstahammar	2.90	4.14	2.43

Table 5. Influence of the heat capacity coefficient *C* on the behavior of the model evaluated for the region of Surahammar on three representative days (January 15–17, 2017). C_0 is the calculated heat capacity coefficient (i.e. baseline, see Table 3), which leads to the parameters presented in **bold**.

C/C_0 [-]	Maximum temperature [°C]	Minimum temperature [°C]	Maximum temperature difference [°C]	Temperature difference variation compared to baseline [%]
0.1	23.57	14.30	9.26	+208
0.2	23.19	15.53	7.66	+148
0.5	21.83	17.33	4.50	+47.4
1	**20.65**	**17.88**	**2.78**	**0**
2	20.21	18.84	1.37	-25.7
5	20.00	19.16	0.84	-59.1
10	20.00	19.63	0.37	-73.7

4. Model validation

The heat transfer coefficients and heat capacity coefficients of the models developed in Section 2 and 3 can be compared and validated with literature data if converted to specific parameters per unit of heated space.

Since the total heated area of the regions of the Västerås DHN is unknown, this is estimated based on the energy statistics published by the Swedish Energy Agency [52]. The document reports the values of the average yearly energy consumption per square meter of heated surface for different Swedish counties. The ratio between the total yearly consumption $Q_{\mathrm{tot,i}}$ of a given region *i* and the average yearly consumption Q_{avg} gives the estimation of the total heated surface of that region, namely $A_{\mathrm{tot,i}}$, as in Eq. (5):

$$A_{\mathrm{tot,i}} = \frac{Q_{\mathrm{tot,i}}}{Q_{\mathrm{avg}}} \tag{5}$$

The model coefficients calculated above are then scaled with this estimation to obtain the specific coefficients per unit of the heated area given by Eqs. (6):

$$U_{A,\mathrm{i}} = \frac{U_{\mathrm{i}}}{A_{\mathrm{tot,i}}} \tag{6a}$$

$$C_{A,\mathrm{i}} = \frac{C_{\mathrm{i}}}{A_{\mathrm{tot,i}}} \tag{6b}$$

By assuming an average height *H* of the heated environments of 3 m, it is possible to further scale the values and obtain the specific coefficients per unit of heated volume U_V and C_V.

$$U_{V,\mathrm{i}} = \frac{U_{A,\mathrm{i}}}{H} \tag{7a}$$

$$C_{V,\mathrm{i}} = \frac{C_{A,\mathrm{i}}}{H} \tag{7b}$$

The statistics for the county of Västmanland, where Västerås is located, present the average yearly heat consumption Q_{avg} between 135 kWh/m^2 and 165 kWh/m^2 [52]. The range of variation with this parameter of the total heated area estimated for the Västerås DHN regions are reported in Table 6.

Table 6. Estimation of the total heat and total heated area of the six regions of the Västerås district heating network.

Region	Q_{tot} [kWh]	A_{tot} [m^2]
Surahammar	$4.18 \cdot 10^7$	$(2.95 \pm 0.14) \cdot 10^5$
Skultuna	$1.90 \cdot 10^7$	$(1.28 \pm 0.13) \cdot 10^5$
Rönnby	$1.22 \cdot 10^7$	$(0.82 \pm 0.08) \cdot 10^5$
Tillberga	$2.02 \cdot 10^7$	$(1.36 \pm 0.13) \cdot 10^5$
Barkarö	$1.22 \cdot 10^7$	$(0.83 \pm 0.09) \cdot 10^5$
Hallstahammar	$1.21 \cdot 10^8$	$(8.15 \pm 0.81) \cdot 10^5$

The sensitivity analysis of the specific coefficients U_V and C_V by varying Q_{avg} within the abovementioned boundaries is shown in Figure 9. The characteristic time of each region τ, obtained as the ratio between the heat capacity and the heat dissipation to the environment, is also represented:

$$\tau_{\mathrm{i}} = \frac{C_{\mathrm{i}}}{U_{\mathrm{i}}} \tag{8}$$

The values of the coefficients U_V and C_V calculated in [49] for individual buildings in the Turin DHN are around 0.85 W/(m^3 °C) and $5 \cdot 10^4$ J/(m^3 °C), respectively. The characteristic times vary significantly depending on building type: most values are around $7 \cdot 10^4$ s, while some are even smaller than $5 \cdot 10^4$ s.

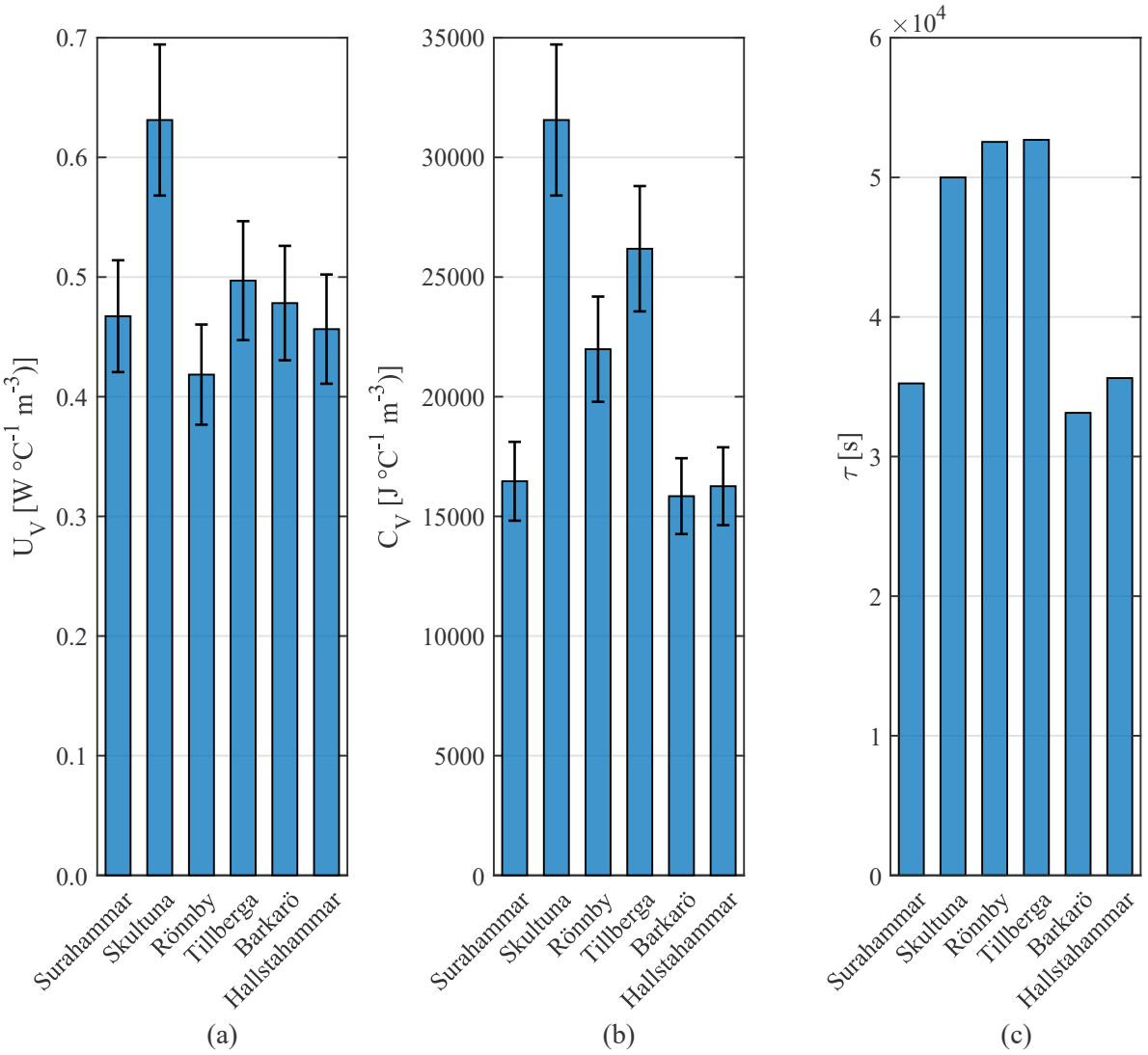

Figure 9. Specific coefficients of heat transfer (a) and heat capacity (b) per unit of heated volume by varying the average yearly consumption, and characteristic time (c).

Even though results obtained in this work are slightly lower than the literature values, they share the same order of magnitude. In addition, the fact that the characteristic times are comparable shows that the heat transfer and heat capacity coefficients are coherent. Moreover, it is worth stating that the literature values have been obtained for individual buildings in the city of Turin, which is characterized by old multi-story dwellings. The regions of Västerås are likely to be characterized by aggregations of newer or more energy-efficient dwellings, therefore a lower loss coefficient can be reasonably expected. This is confirmed by a research stating that the average temperature loss of Italian houses – when the indoor and outdoor temperatures are 20 °C and 0 °C, respectively – is 1.5

°C, while in Sweden this parameter drops to 1.2 °C [53]. Hence, lower values of the heat loss coefficient for networks in Sweden compared to Italy are justified by the different characteristics of the connected buildings. Additionally, another paper [40] reports that the values of the internal heat capacity of light-weight buildings drop to $8 \cdot 10^4$ J/(m^2 °C), which corresponds to around $3 \cdot 10^4$ J/(m^3 °C) and is coherent with the analysis in Figure 9.

A further check with the considerations drawn in [41] is represented in Figure 10. According to Leśko *et al.*, the aggregated DSM actions performed (i.e. storage of thermal energy in consumer capacity) are limited to 1.4 % of the total heat demand [41] in the period analyzed. The potential daily heat storage obtained with this assumption can be compared with that obtained with the model proposed in this work. In this case, the energy stored is calculated as:

$$Q_{\text{stored}} = C\Delta T_{\max} \tag{9}$$

where $\Delta T_{\max}$ is the maximum acceptable variation in indoor temperature compared to the required set-point, considered equal to ± 0.5 °C. The results obtained are comparable also in this case.

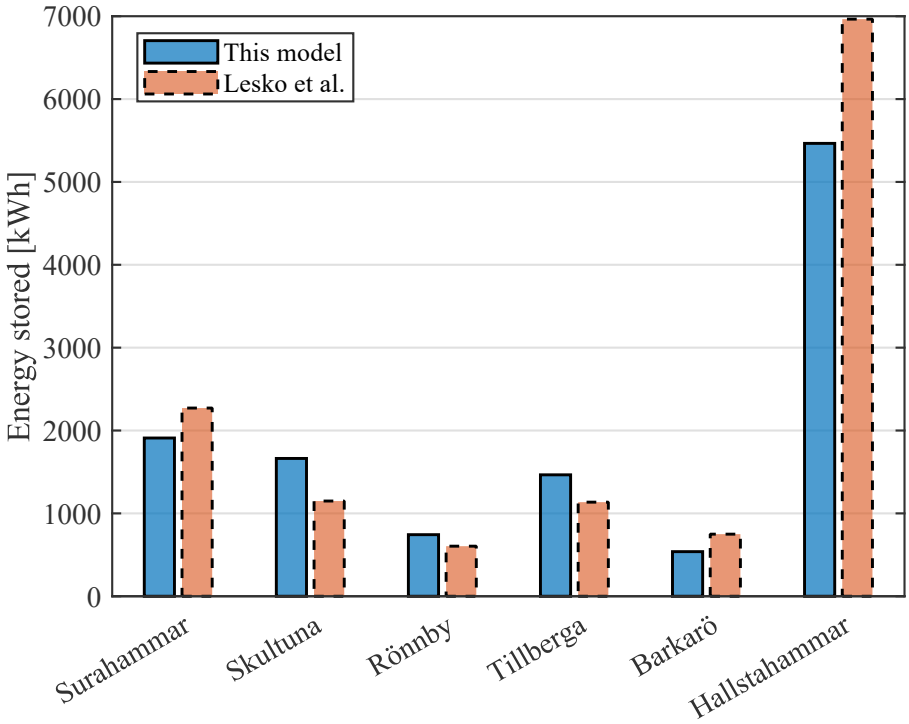

Figure 10. Energy stored in the region's thermal capacity: comparison between this model and that proposed by Leśko *et al.* [41].

Finally, a preliminary test of the model feasibility for DSM is carried out by means of a simple application in the Simulink® environment [54]. Thermal power supply – available from the historical data – from the substation heat exchanger to the model of the aggregated consumer is simulated and the equivalent indoor temperature of the aggregated consumer is then visualized. An exemplifying result concerning the region of Surahammar for the heating season from October 2018 to March 2019 is depicted in Figure 11. It can be noted that the estimated U and C are reliable, as the simulated behavior is plausible and does not diverge in the long-term. Indeed, the model temperature is kept around 21 °C and is subject to daily variations between 2 °C to 4 °C, which is compatible with the expected profile. Additional weekly periodical variations in the temperature evolution can be noticed and justified by the different behavior typically observed on weekends and during holidays (when commercial, industrial or tertiary-sector end-users seldom require heating). This has an influence on the temperature of the aggregated region, which is a representation of its energy content.

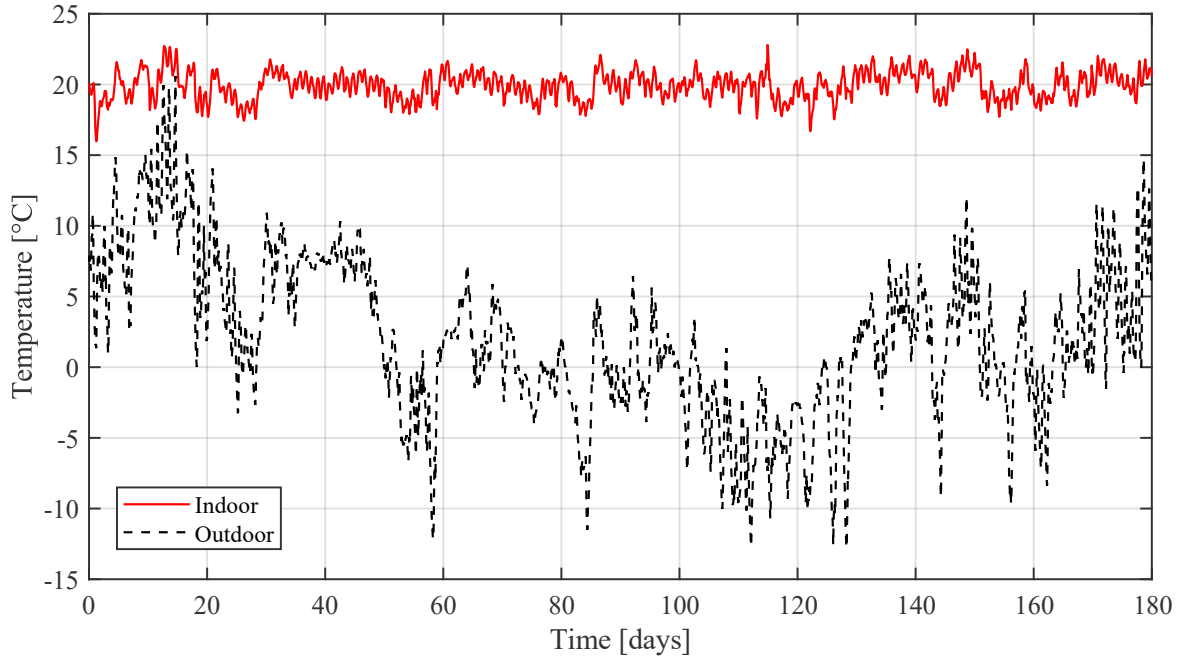

Figure 11. Preliminary test of the model performed with a Simulink® application [54]. The results of the indoor temperature refer to the region of Surahammar during the heating season from October 2018 to March 2019.

5. Discussion

The presented model of a DHN aggregated region can be used for several applications, since it has the following advantages:

- The model provides an estimation of the heat capacity of the buildings connected to a given substation as an aggregated consumer and, therefore, paves the way for its exploitation as thermal storage. It should be noted that most state-of-the-art models of DHNs consider the multiplicity of consumers as an external element which acts on the network by imposing a heat demand that cannot be varied.
- In this regard, the heat capacity coefficient can be used to provide insights on the heat storage potential of a given region or set of consumers to enable DSM options. Assuming that the heat demand of a region (obtained from historical data or forecasted) is able to keep the indoor thermal comfort of the consumers in that region, for instance by maintaining the indoor set-point temperature, and considering a suitable temperature deviation from that set-point, it is possible to calculate the amount of heat that can be stored over a given time period without altering user comfort perception (Eq. (9)). The potential heat storage capacity achievable with an indoor temperature deviation of ±0.5 °C for the Västerås regions is illustrated in Figure 12. The graph shows similar results to those presented in [31], which concern the estimation of building demand response potential.
- The exploitation of the regions as thermal storage allows DSM strategies such as peak shaving to be implemented without requiring the installation of dedicated storage devices, the cost-effectiveness of which should be carefully evaluated by the system operator.
- This model is able to aggregate several buildings connected to a substation only requiring basic data on energy flows, without the need to carry out a time-consuming evaluation of the building types and characteristics, which may introduce errors and inaccuracies. This is different from many literature models, which manage the heat storage potential starting from

archetypes or individual building characterization and, therefore, cannot easily extend smart management and control solutions to large-scale networks.

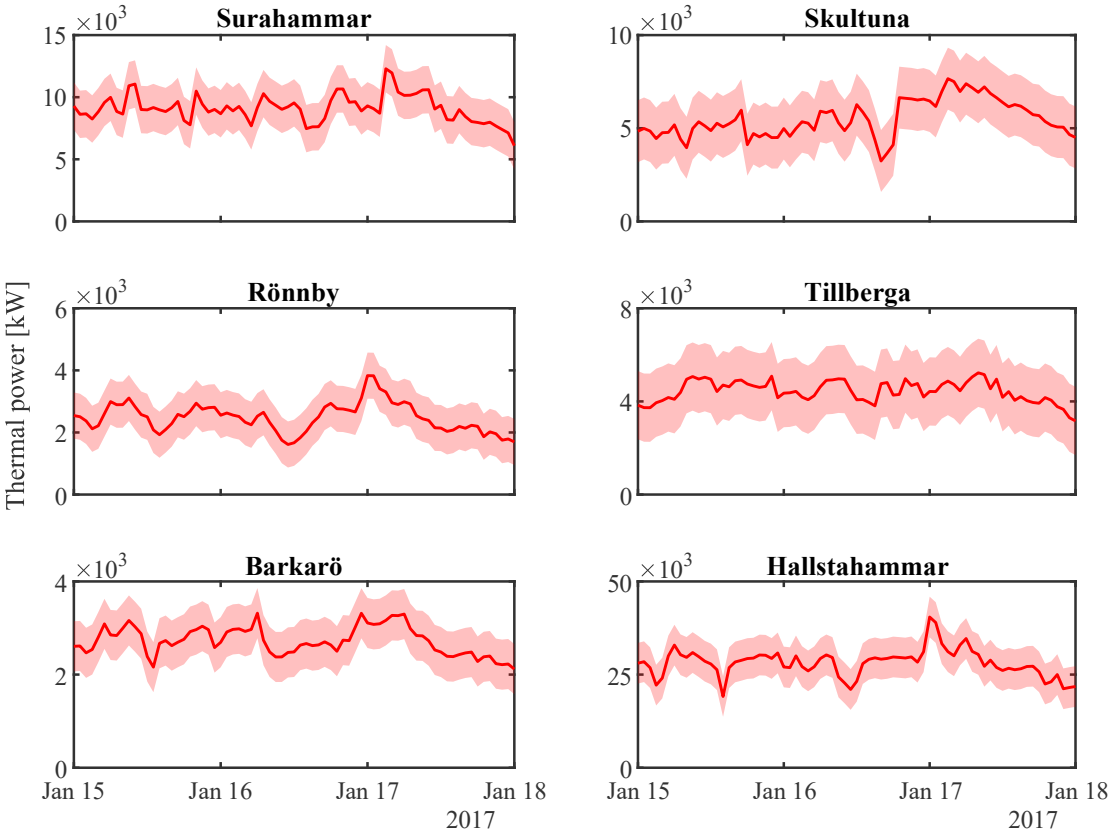

Figure 12. Heat storage potential of the six regions. The full line represents the historical thermal power, while the shaded area represents the heat that can be stored each hour by considering an indoor temperature deviation of 0.5 °C.

- The model is scale-free and can applied to any part of the system for which data are available. The described approach does not depend on the number of buildings or on the focus area, thus it is valid for a city as well as for an individual building. The characteristics of the region constituents, which influence the collected dataset, are directly reflected and included in the results of the model identification procedure. In addition, the procedure is fast and easily replicable by the utilities of several heating networks, without needing specific modeling competences or system knowledge with a fine granularity.

- Due to the simplified approach used in its development, the proposed model can be easily exploited in Linear Programming optimization problems, for which practical and fast software solutions are available [55].
- In the presented procedure, an increase in system size does not correspond to an exponential increase in optimization complexity. The model is therefore particularly suitable for unlocking the potential of Model Predictive Control, where computational speed is of primary importance. MPC implements optimal control with a receding time horizon strategy, updating the system state and model variables and repeating the online optimization at every given time interval [56]. Hence, the simplifications of the proposed model are effectively counterbalanced by this periodic feedback, which allows modeling inaccuracies to be rejected.

As previously mentioned, the demonstration of MPC for achieving demand side management in an entire DHN with this model was successful in [46].

A potential limitation of the presented model can be identified in the low level of detail in representing individual buildings, as they are clustered with equivalent parameters and properties. Nevertheless, the experimental definition of a significant value of the actual indoor temperature of the buildings in large-scale DHNs is not straightforward and a management solution based on its detailed monitoring may not be applicable. Hence, a region-level view can be beneficial, especially in real-time control applications of the distribution network. Moreover, the conservative estimation of the heat storage potential leads to a negligible risk of jeopardizing end-user comfort.

Future developments of the study will be dedicated to a further validation of the model on controlled small-scale and large-scale real demonstrators. Measurement devices will be installed, the indoor temperature will be monitored, and experimental tests will be conducted on DHN portions of different sizes.

6. Conclusions

The currently available models of large-scale district heating networks do not allow the thermal capacity of the connected end-users to be efficiently included in system optimization and real-time control. Indeed, typically the inclusion of thermal mass relies either on indoor temperature monitoring (which is rarely available in large-scale heating networks) or on a detailed knowledge of the characteristics of the buildings (e.g. time constants, materials and size) and, therefore, this is time-consuming and daunting for large-scale applications. This work proposed a method that can be readily applied using a potentially small amount of data usually accessible to district heating providers. Starting from the data available at the main substation heat exchangers of the peripheral regions of the district heating network of Västerås, Sweden, a physics-based equivalent model of each aggregated region was identified and validated with data from the literature and simulations. Additionally, sensitivity analysis was carried out to further show the robustness and reliability of the procedure, and its potential replicability to different substations. The model was exploited to evaluate the aggregated storage potential of the regions and will be the key element of smart optimization and control strategies. Indeed, the model is ideal for implementing demand side management, e.g. shaving the peaks of thermal energy distribution, and for setting up real-time predictive controllers. Thus, the proposed complete procedure will provide valuable tools for the digitalization of district heating and sustainable energy transition.

Acknowledgements

This work was supported by the "DISTRHEAT – Digital Intelligent and Scalable conTrol for Renewables in HEAting neTworks" project, which received funding in the framework of the joint programming initiative ERA-Net Smart Energy Systems' focus initiative Integrated, Regional Energy Systems, with support from the European Union's Horizon 2020 research and innovation programme under grant agreement No 775970. It was also supported by the "Bando Leonardo da Vinci 2019 – Azione 2" funded by the Italian Ministry of Education, University and Research (MIUR).

The authors would also like to thank their industrial partner Mälarenergi AB for providing the data of the district heating network of Västerås.

References

[1] Communication from the Commission to the European Parliament, the European Council, the Council, the European Economic and Social Committee, the Committee of the Regions and the European Investment Bank. A Clean Planet for all a European strategic long-term vision for a prosperous, modern, competitive and climate neutral economy. COM/2018/773. Brussels, 28/11/2018. Available at: https://eur-lex.europa.eu/legal-content/EN/TXT/?uri=CELEX:52018DC0773 [accessed on 15/09/2021]

[2] Werner S. International review of district heating and cooling. Energy 2017;137:617–631. https://doi.org/10.1016/j.energy.2017.04.045

[3] Paardekooper S, Lund RS, Mathiesen BV, Chang M, Petersen UR, Grundahl L, David A, Dahlbaek J, Kapetanakis IA, Lund H, Bertelsen N, Hansen K, Drysdale DW, Persson U. Heat Roadmap Europe Quantifying the Impact of Low-carbon Heating and Cooling Roadmaps. Technical report, Aalborg Universitetsforlag, 2018. https://vbn.aau.dk/en/publications/heat-roadmap-europe-4-quantifying-the-impact-of-low-carbon-heatin

[4] Saletti C, Morini M, Gambarotta A. The Status of Research and Innovation on Heating and Cooling Networks as Smart Energy Systems within Horizon 2020. Energies 2020;13(11):2835. https://doi.org/10.3390/en13112835

[5] Sernhed K, Lygnerud K, Werner S. Synthesis of recent Swedish district heating research. Energy 2018;151:126–132. https://doi.org/10.1016/j.energy.2018.03.028

[6] Leoni P, Geyer R, Schmidt RR. Developing innovative business models for reducing return temperatures in district heating systems: Approach and first results. Energy 2020;195:116963. https://doi.org/10.1016/j.energy.2020.116963

[7] Jebamalai JM, Marlein K, Laverge J, Vandevelde L, van den Broek M. An automated GIS-based planning and design tool for district heating: Scenarios for a Dutch city. Energy 2019;183: 487–496. https://doi.org/10.1016/j.energy.2019.06.111

[8] Nguyen T, Gustavsson L. Production of district heat, electricity and/or biomotor fuels in renewable-based energy systems. Energy 2020;202:117672. https://doi.org/10.1016/j.energy.2020.117672

[9] Prina MG, Manzolini G, Moser D, Nastasi B, Sparber W. Classification and challenges of bottom-up energy system models - A review. Renewable and Sustainable Energy Reviews 2020;129:109917. https://doi.org/10.1016/j.rser.2020.109917

[10] Hoyo Arce Id, Herrero López S, López Perez S, Rämä M, Klobut K, Febres JA. Models for fast modelling of district heating and cooling networks. Renewable and Sustainable Energy Reviews 2018;82: 1863–1873. https://doi.org/10.1016/j.rser.2017.06.109

[11] Ma W, Fang S, Liu G, Zhou R. Modeling of district load forecasting for distributed energy system. Applied Energy 2017;204:181–205. https://doi.org/10.1016/j.apenergy.2017.07.009

[12] Mustafaraj G, Marini D, Costa A, Keane M. Model calibration for building energy efficiency simulation. Applied Energy 2014;130:72–85. https://doi.org/10.1016/j.apenergy.2014.05.019

[13] Kim EJ, Plessis G, Hubert JL, Roux JJ. Urban energy simulation: Simplification and reduction of building envelope models. Energy and Buildings 2014;84:193–202. https://doi.org/10.1016/j.enbuild.2014.07.066

[14] Famuyibo AA, Buffy A, Strachan P. Developing archetypes for domestic dwellings—An Irish case study. Energy and Buildings 2012;50:150–157. https://doi.org/10.1016/j.enbuild.2012.03.033

[15] Coakley D, Raftery P, Keane M. A review of methods to match building energy simulation models to measured data. Renewable and Sustainable Energy Reviews 2014;37:123–141. https://doi.org/10.1016/j.rser.2014.05.007

[16] Lundström L, Akander J, Zambrano J. Development of a Space Heating Model Suitable for the Automated Model Generation of Existing Multifamily Buildings—A Case Study in Nordic Climate. Energies 2019; 12(3), 485. https://doi.org/10.3390/en12030485

[17] Fonseca JA, Schlueter A. Integrated model for characterization of spatiotemporal building energy consumption patterns in neighborhoods and city districts. Applied Energy 2015;142:247–265. https://doi.org/10.1016/j.apenergy.2014.12.068

[18] Marquant JF, Bollinger LA, Evins R, Carmeliet J. A new combined clustering method to Analyse the potential of district heating networks at large-scale. Energy 2018;156:73–83. https://doi.org/10.1016/j.energy.2018.05.027

[19] Omu A, Choudhary R, Boies A. Distributed energy resource system optimisation using mixed integer linear programming. Energy Policy 2013;61:249–266. https://doi.org/10.1016/j.enpol.2013.05.009

[20] Dominković DF, Stunjek G, Blanco I, Madsen H, Krajačić G. Technical, economic and environmental optimization of district heating expansion in an urban agglomeration. Energy 2020;197:117243. https://doi.org/10.1016/j.energy.2020.117243

[21] Kannengießer T, Hoffmann M, Kotzur L, Stenzel P, Schuetz F, Peters K, Nykamp S, Stolten D, Robinius M. Reducing Computational Load for Mixed Integer Linear Programming: An Example for a District and an Island Energy System. Energies 2019, 12, 2825. https://doi.org/10.3390/en12142825

[22] Müller A, Hummel M, Kranzl L, Fallahnejad M, Büchele R. Open Source Data for Gross Floor Area and Heat Demand Density on the Hectare Level for EU 28. Energies 2019, 12, 4789. https://doi.org/10.3390/en12244789

[23] Chertkov M, Novitsky NN. Thermal Transients in District Heating Systems. Energy 2019;184:22–33. https://doi.org/10.1016/j.energy.2018.01.049

[24] Larsen HV, Bøhm B, Wigbels M. A comparison of aggregated models for simulation and operational optimisation of district heating networks. Energy Conversion and Management 2004;45:1119–1139. https://doi.org/10.1016/j.enconman.2003.08.006

[25] Guelpa E, Verda V. Compact physical model for simulation of thermal networks. Energy 2019;175: 998–1008. https://doi.org/10.1016/j.energy.2019.03.064

[26] Zajacs A, Borodiņecs A. Assessment of development scenarios of district heating systems. Sustainable Cities and Society 2019;48:101540. https://doi.org/10.1016/j.scs.2019.101540

[27] Sommer T, Sulzer M, Wetter M, Sotnikov A, Mennel S, Stettler C. The reservoir network: A new network topology for district heating and cooling. Energy 2020;199: 117418. https://doi.org/10.1016/j.energy.2020.117418

[28] Leitner B, Widl E, Gawlik W, Hofmann R. A method for technical assessment of power-to-heat use cases to couple local district heating and electrical distribution grids. Energy 2019;182:729–738. https://doi.org/10.1016/j.energy.2019.06.016

[29] Reynders G, Nuytten T, Saelens D. Potential of structural thermal mass for demand-side management in dwellings. Building and Environment 2013;64:187–199. https://doi.org/10.1016/j.buildenv.2013.03.010

[30] Ma Z, Knotzer A, Billanes JD, Jørgensen BN. A literature review of energy flexibility in district heating with a survey of the stakeholders' participation. Renewable and Sustainable Energy Reviews 2020;123:109750. https://doi.org/10.1016/j.rser.2020.109750

[31] Yin R, Kara EC, Li Y, DeForest N, Wang K, Yong T, Stadler M. Quantifying flexibility of commercial and residential loads for demand response using setpoint changes. Applied Energy 2016;177: 149–164. https://doi.org/10.1016/j.apenergy.2016.05.090

[32] Kouhia M, Laukkanen T, Holmberg H, Ahtila P. District heat network as a short-term energy storage. Energy 2019;177:292–303. https://doi.org/10.1016/j.energy.2019.04.082

[33] Sartor K, Dewallef P. Integration of heat storage system into district heating networks fed by a biomass CHP plant. Journal of Energy Storage 2018;15:350–358. https://doi.org/10.1016/j.est.2017.12.010

[34] Foteinaki K, Li R, Péan T, Rode C, Salom J. Evaluation of energy flexibility of low-energy residential buildings connected to district heating. Energy and Buildings 2020;213:109804. https://doi.org/10.1016/j.enbuild.2020.109804

[35] Dominković DF, Gianniou P, Münster M, Heller A, Rode C. Utilizing thermal building mass for storage in district heating systems: Combined building level simulations and system level optimization. Energy 2018;153:949–966. https://doi.org/10.1016/j.energy.2018.04.093

[36] Kensby J, Trüschel A, Dalenbäck JO. Potential of residential buildings as thermal energy storage in district heating systems – Results from a pilot test. Applied Energy 2015;137:773–781. https://doi.org/10.1016/j.apenergy.2014.07.026

[37] Romanchenko D, Kensby J, Odenberger M, Johnsson F. Thermal energy storage in district heating: Centralised storage vs. storage in thermal inertia of buildings. Energy Conversion and Management 2018;162:26–38. https://doi.org/10.1016/j.enconman.2018.01.068

[38] Bhattacharya S, Chandan V, Arya V, Kar K. DReAM: Demand Response Architecture for Multi-level District Heating and Cooling Networks. Proceedings of the 8th International Conference on Future Energy Systems (e-Energy '17), May 16-19, 2017, Shatin, Hong Kong, 353–359. https://doi.org/10.1145/3077839.3084079

[39] Bhattacharya S, Chandan V, Arya V, Kar K. Demand Response for Thermal Fairness in District Heating Networks. IEEE Transactions on Sustainable Energy 2019;10(2):865–875. https://doi.org/10.1109/TSTE.2018.2852629

[40] Turski M, Sekret R. Buildings and a district heating network as thermal energy storages in the district heating system. Energy and Buildings 2018;179:49–56. https://doi.org/10.1016/j.enbuild.2018.09.015

[41] Leśko M, Bujalski W, Futyma. Operational optimization in district heating systems with the use of thermal energy storage. Energy 2018;165:902–915. https://doi.org/10.1016/j.energy.2018.09.141

[42] Sun C, Chen J, Cao S, Gao X, Xia G, Qi C, Wu X. A dynamic control strategy of district heating substations based on online prediction and indoor temperature feedback. Energy 2021;235:121228. https://doi.org/10.1016/j.energy.2021.121228

[43] Hering D, Cansev ME, Tamassia E, Xhonneux A, Müller D. Temperature control of a low-temperature district heating network with Model Predictive Control and Mixed-Integer Quadratically Constrained Programming. Energy 2021;224:120140. https://doi.org/10.1016/j.energy.2021.120140

[44] Knudsen BR, Rohde D, Kauko H. Thermal energy storage sizing for industrial waste-heat utilization indistrict heating: A model predictive control approach. Energy 2021;234:121200. https://doi.org/10.1016/j.energy.2021.121200

[45] Kotzur L, Nolting L, Hoffmann M, Gross T, Smolenko A, Priesmann J, Büsing H, Beer R, Kullmann F, Singh B, Praktiknjo A, Stolten D, Robinius M. A modeler's guide to handle complexity in energy systems optimization. Advances in Applied Energy 2021;4:1000063. https://doi.org/10.1016/j.adapen.2021.100063

[46] Saletti C, Zimmerman N, Morini M, Kyprianidis K, Gambarotta A. Enabling smart control by optimally managing the State of Charge of district heating networks. Applied Energy 2021;283:116286. https://doi.org/10.1016/j.apenergy.2020.116286

[47] Calikus E, Nowaczyk S, Sant'Anna A, Gadd H, Werner S. A data-driven approach for discovering heat load patterns in district heating. Applied Energy 2019;252:113409. https://doi.org/10.1016/j.apenergy.2019.113409

[48] Unternährer J, Moret S, Joost S, Maréchal F. Spatial clustering for district heating integration in urban energy systems: Application to geothermal energy. Applied Energy 2017;190:749–763. https://doi.org/10.1016/j.apenergy.2016.12.136

[49] Guelpa E, Deputato S, Verda V. Thermal request optimization in district heating networks using a clustering approach. Applied Energy 2018;228:608–617. https://doi.org/10.1016/j.apenergy.2018.06.041

[50] Nageler P, Heimrath R, Mach T, Hochenauer. Prototype of a simulation framework for georeferenced large-scale dynamic simulations of district energy systems. Applied Energy 2019;252:113469. https://doi.org/10.1016/j.apenergy.2019.113469

[51] Månsson S, Lundholm Benzi I, Thern M, Salenbien R, Sernhed K, Johansson Kallioniemi PO. A taxonomy for labeling deviations in district heating customer data. Smart Energy 2021;2:100020. https://doi.org/10.1016/j.segy.2021.100020

[52] Energistatistik för flerbostadshus 2016 (Energy statistics for multi-dwelling buildings in 2016). Sveriges officiella statistik. Swedish Energy Agency ES 2017:4. ISSN 1654-7543 [available in Sweden]

[53] Guidebook. UK homes losing heat up to three times faster than European neighbours. February 20, 2020. Available at https://www.tado.com/t/en/uk-homes-losing-heat-up-to-three-times-faster-than-european-neighbours/ [accessed on 15/09/2021]

[54] Cadau N, De Lorenzi A, Gambarotta A, Morini M, Saletti C. A Model-in-the-Loop application of a Predictive Controller to a District Heating system. Energy Procedia 2018;148:352–359. https://doi.org/10.1016/j.egypro.2018.08.088

[55] Gearhart JL, Adair KL, Detry RJ, Durfee JD, Jones KA, Martin N. Comparison of Open-Source Linear Programming Solvers. Sandia National Laboratories, Sandia Report SAND2013-8847, October 2013. Available online at: https://prod-ng.sandia.gov/techlib-noauth/access-control.cgi/2013/138847.pdf [accessed on 03/07/2020]

[56] De Lorenzi A, Gambarotta A, Morini M, Rossi M, Saletti C. Setup and testing of smart controllers for small-scale district heating networks: an integrated framework. Energy 2020;205:118054. https://doi.org/10.1016/j.energy.2020.118054

Nomenclature

A_{tot}	total heated area [m^2]
C	aggregated heat capacity coefficient [kJ °C^{-1}]
c	water specific heat capacity [kJ kg^{-1} °C^{-1}]
f	flag variable for meeting acceptability band constraints [-]
H	average height of heated environment [m]
J	cost function [°C h]
$\dot{m}$	mass flow rate [kg s^{-1}]
$\dot{Q}$	thermal power [kW]
Q	heat [kJ]
Q_{avg}	average yearly heat consumption [kWh m^{-2}]
Q_{tot}	total yearly heat consumption [kWh]
T	temperature [°C]
t	time [s]
U	aggregated heat transfer coefficient [kW °C^{-1}]
ϕ	penalty factor for violation of acceptability band constraints [°C s]
τ	characteristic time [s]

Subscripts

A	specific per unit of heated area
ext	outdoor

i	region *i*
k	day *k*
max	maximum
min	minimum
R	return
S	supply
SP	set-point
stored	stored
V	specific per unit of heated volume

Acronyms

CHP	Combined Heat and Power
DHN	District Heating Network
DSM	Demand Side Management
MILP	Mixed Integer Linear Programming
MPC	Model Predictive Control